Manuscript Details

Manuscript number	DSR2_2019_196
Title	Ocean currents and environmental gradients in the vicinity of the Madagascar Ridge in the Southwest Indian Ocean
Article type	Full length article

Abstract

As a 1 300 km longitudinally submerged extension of Madagascar, the Madagascar Ridge is a significant feature in the Southwest Indian Ocean. The ridge rises from abyssal depths to around 2000 m with several shallow (750-20m) seamounts occupying the northern and southern regions. Certainly the Walters Shoal is becoming recognised as a biological hotspot. The orientation of the ridge means that it traverses the background westward re-circulation of the Southwest Indian Ocean sub-gyre that apparently contributes to the Agulhas Current on the east coast of southern Africa. Because of its remoteness, little is known of the ridge's role in the local and regional oceanography and biology — although tuna fisheries operate in the north and around the Walters Shoal farther south. This remoteness has led to few in situ measurements having been made in the vicinity of the Madagascar Ridge. In this context, our study provides the first detailed description of the wind field and ocean properties along the Madagascar Ridge. In particular the study aims to provide a backdrop for several new investigations that focus on an unnamed seamount (260 m) on the northern sector of the ridge and the Walters Shoal (20 m) in the south. Spatial fields and along-ridge gradients of surface wind, SST, MLD, EKE, Heat Flux and Chl-a are produced to help biologists understand biological ramifications. These reveal contrasting environments between the northern and southern regions of the ridge. To gain an understanding of the circulation dynamics along the 1300 km long ridge and connectivity in the region — a novel approach of 'virtual moorings' is used. These comprised selected positions along the ridge with the compilation of 4-year long time series of satellite-derived geostrophic currents. It is shown that currents (and EKE) decrease from north to south with greater variability. The northern ridge is highly dynamic due to the presence of the East Madagascar Current and its retroflection into the East Madagascar Return Current. By comparison, Walters Shoal in the south is in a quiescent zone.

Corresponding Author	Patrick Vianello
Corresponding Author's Institution	Nelson Mandela University
Order of Authors	Patrick Vianello, Ternon Jean-Francois, Steven Herbette, Hervé DEMARCQ, Michael Roberts

Submission Files Included in this PDF

File Name [File Type]

Paper 2 Final version MJR (004).docx [Manuscript File]

Figurespaper2.pdf [Figure]

Paper 2_Authors'Declaration of Interest.docx [Conflict of Interest]

Ocean currents and environmental gradients in the vicinity of the Madagascar Ridge in the Southwest Indian Ocean

Authors: Patrick Vianello[a,*], Jean-Francois Ternon[b], Herve Demarcq[b], Steven Herbette[c], Michael Roberts[a,d]

a. *Ocean Science & marine Food Security, Nelson Mandela University, Port Elizabeth, South Africa*
b. *MARBEC, IRD, Univ Montpellier, CNRS, Ifremer, Sète, France*
c. *Laboratoire d'Océanographie Physique et Spatiale (LOPS), IUEM, Univ. Brest - CNRS - IRD - Ifremer, Brest, France*
d. *National Oceanography Centre, Southampton, United Kingdom*

* *Corresponding author: patrick.vianello2@gmail.com*

ABSTRACT

As a 1 300 km longitudinally submerged extension of Madagascar, the Madagascar Ridge is a significant feature in the Southwest Indian Ocean. The ridge rises from abyssal depths to around 2000 m with several shallow (750-20m) seamounts occupying the northern and southern regions. Certainly the Walters Shoal is becoming recognised as a biological hotspot. The orientation of the ridge means that it traverses the background westward re-circulation of the Southwest Indian Ocean sub-gyre that apparently contributes to the Agulhas Current on the east coast of southern Africa. Because of its remoteness, little is known of the ridge's role in the local and regional oceanography and biology — although tuna fisheries operate in the north and around the Walters Shoal farther south. This remoteness has led to few in situ measurements having been made in the vicinity of the Madagascar Ridge. In this context, our study provides the first detailed description of the wind field and ocean properties along the Madagascar Ridge. In particular the study aims to provide a backdrop for several new investigations that focus on an unnamed seamount (260 m) on the northern sector of the ridge and the Walters Shoal (20 m) in the south. Spatial fields and along-ridge gradients of surface wind, SST, MLD, EKE, Heat Flux and Chl-a are produced to help biologists understand biological ramifications. These reveal contrasting environments between the northern and southern regions of the ridge. To gain an understanding of the circulation dynamics along the

1300 km long ridge and connectivity in the region — a novel approach of ‘virtual moorings’ is used. These comprised selected positions along the ridge with the compilation of 4-year long time series of satellite-derived geostrophic currents. It is shown that currents (and EKE) decrease from north to south with greater variability. The northern ridge is highly dynamic due to the presence of the East Madagascar Current and its retroflection into the East Madagascar Return Current. By comparison, Walters Shoal in the south is in a quiescent zone.

Key words: Madagascar Ridge, seamounts, Walters Shoal, SST, EKE, geostrophic currents

1. Introduction

1.1. Madagascar Ridge and significance

The Madagascar Ridge in the south-western Indian Ocean is a significant bathymetric feature that has received little scientific attention. Aligned longitudinally, it extends south of the Madagascar landmass for some 1 300 km (~10 degrees of latitude; Figs. 1 and 2) with a width of approximately 400 km. Water depths over much of the plateau are between 2 and 3 km. The southern half of the ridge rises to the prominent Walters Shoal seamount that comes within 20 m of the surface. The flat summit is covered with coral reefs with broken and jagged relief, especially along the outer edges. Walters Shoal is amongst a group of several deeper seamounts. The northern part of the Ridge likewise comprises a cluster of seamounts that are shallower than 750 m. One of these, referred to in this study as the Mad-ridge seamount, rises to a depth of 260 m below the sea surface (27.5° S 46.25° E; see Roberts et al., this issue). The western side of the ridge comprises a steep scarp that runs down into the 5 km-deep Mozambique basin. The slope of the eastern flank is more gentle, leading into the 5-6 km-deep Madagascar basin. South of Walters Shoal the water depth increases rapidly to more than 3 km, where upon, the 4 km isobath joins the Southwest Indian Ridge.

Even with the northern and southern seamount clusters highlighted in Fig 2b, the ridge is mostly flat-topped and covered by 0.5–1.0 km of undisturbed sediments (Goslin et al. 1980). Original work by Sinha et al. (1981) considers the Madagascar Ridge to be an aseismic plateau separating two ocean basins of mid- to late Cretaceous age. From interpretations of a reversed refraction line on the ridge and a continuous trans gravity profile, they concluded that the Ridge was formed during the Cretaceous as thickened oceanic crust at a mid-ocean ridge which possibly overlies a mantle hot-spot. It is possible that the Madagascar Ridge is the northern analogue of the Crozet plateau and owes its origin to the excess volcanism of the Prince Edward Island hotspot (Morgan 1972).

The importance of the Madagascar Ridge is still being discovered. While the deep ridge itself is perhaps of lesser direct biologically significance (this still needs to be confirmed), the shallow Walters Shoal has received ample attention from fishing fleets and recreational fishing expeditions (Parin et al., 1993). On the northern ridge, tuna fishing and the abundant bird activity point to a productive hotspot (Pinet et al., 2012). With a range of over 10 degrees in the mid latitudes and a N-S orientation — the Madagascar Ridge is destined to experience starkly contrasting environments that no doubt shape its biology and connectivity to the greater SWIO, including the extensive Agulhas Current system. Moreover, as a prominent bathymetric feature, the ridge — especially in the north — appears to be a major source of internal waves that in part promote productivity there (Buijsman et al., 2016; Sangra et al., 2001). This source of internal waves could also have distant consequences such as interactions with internal waves generated at the Sofala Bank (da Silva et al., 2009). While oceanographic knowledge exists for the regions south, west and east of Madagascar (i.e. the EMC, Mozambique Channel, and SICC (de Ruijter et al., 2004; Siedler et al., 2009; Ridderinkhof et al., 2013)) and to the very south in the vicinity of the STF and the Agulhas Return Current — there is little that focuses on the Madagascar Ridge, in particular a description of the annual climate, ocean properties and ocean circulation there. This is particularly important for Madagascar that has an extended EEZ claim on the Ridge, but has no means of obtaining information.

1.2 Recirculation in the South West Indian Ocean sub-gyre

It is accepted that the Subtropical Gyre of the South Indian Ocean forms the general background circulation in the vicinity of the Madagascar Ridge (Fig. 1b). The gyre comprises the Agulhas Current as the major Western Boundary Current which, after retroflecting at the southern tip of Africa, mostly flows back eastwards undergoing a series of semi-permanent meanders between 37°S and 41°S just north of the STF (Subtropical Front). This eastward flow is referred to as the Agulhas Return Current (ARC). The ARC weakens towards the east as transport peels off to the north (Lutjeharms, 2007; Stramma and Lutjeharms, 1997) and then westwards to close the anticyclonic Southwest Indian Ocean Sub-gyre. Pollard and Read (2015) suggest this only begins east of 50°E as estimates of full depth ARC transport (i.e., 84, 71, 73 and 85 Sv at 41°, 42°, 45° and 50°E, respectively) closely match published estimates of the Agulhas Current transport of 73 Sv (Beal and Bryden, 1999), 85 Sv (Toole and Warren, 1993) and 70 ± 21 Sv (Bryden et al., 2005). This differs from earlier work by Lutjeharms and Ansorge (2001). Belkin and Gordon (1996) tracked the ARC up to 75°E. Northward leakage from the ARC also occurs from cyclonic eddies that regularly break off on the north edge of the ARC (reference).

Closure of the Subtropical Gyre has not been completely resolved (Pollard and Read, 2015). There appears to be three main sources for the Agulhas Current: (1) southward flow through the Mozambique Channel, (2) south-westward flow east of Madagascar, i.e. East Madagascar

Current (EMC), and (3) westward flow between Madagascar and the ARC (i.e. over the Madagascar Ridge). de Ruijter et al. (2004, 2005) have shown that the first two sources comprise eddies and dipoles that contribute about 25 Sv to the Agulhas transport (Lutjeharms, 2007; Stramma and Lutjeharms, 1997).

The third Agulhas source — the westward flow between Madagascar and the ARC — is the least studied and the largest, estimated to be 35–40 Sv in the upper 1000 m (Lutjeharms., 2007). Satellite altimetry data (AVISO) show clear westward propagation of eddies (Boebel et al., 2003; Quartly et al., 2006; Schouten et al., 2002) rather than Rossby waves (Chelton et al., 2011). Eddy propagation speeds are larger than Rossby waves (Killworth et al., 1997). Between latitudes 27–33°S, westward propagation is apparent at all longitudes, but volume flux is greater in the north where the EMC generates eddies (of both polarities) (Vianello et al., this issue).

1.3 Northern Ridge

The circulation south of Madagascar on the northern part of the Madagascar ridge is complex, dynamic and not fully understood (Pollard and Read, 2017). Distinct features occur at the termination of the EMC. From hydrography and satellite observations, Lutjeharms et al. (2007) suggested that the EMC behaves in a similar manner as the Agulhas Current and undergoes an eastward retroflection once it becomes a free jet. Lutjeharms et al. (1981) noted the westward propagation of mesoscale eddies south of Madagascar. de Ruiter et al. (2004) demonstrated that much of this turbulence is in the form of dipole eddies which form in the EMC retroflection region and continue to the Agulhas Current. Quartly et al., 2006 suggested that the retroflection at the termination of the EMC is not a permanent feature, unlike the Agulhas retroflection. Siedler et al., (2006, 2009) using climatological altimetry data, proposed the South Indian Ocean Counter-current (SICC) was an eastward extension of the EMC retroflection — also referred to the East Madagascar Return Current (EMRC). Palastanga et al. (2007) observed the SICC to extend to 100°E. Siedler et al. (2009) suggested that up to 40% of the SICC waters originate from the EMC and that almost half of the EMC volume flux contributes to the greater Agulhas Current system.

Coastal upwelling also occurs off the south-eastern coast of Madagascar where the very narrow eastern shelf meets the expansive southern shelf region. Satellite observations show persistent patches of colder water rich in Chl a (e.g. Lutjeharms and Machu, 2000; Roberts et al. (this issue)). This nutrient-rich water is at times observed to be drawn off the shelf by passing eddies (Vianello et al., this issue) and to frequent the northern reaches of the Madagascar Ridge.

1.4 Southern Ridge

Little is known about the circulation south of the EMC retroflection area. There is also confusion. Volume transport calculations show the ocean circulation is influenced by the Southwest Indian subgyre (Fig.1). In the upper 1000 m just north of the STF the eastward transport of the South Indian Ocean Current (SIOC) starts with 60 Sv southeast of South Africa (Stramma and Lutjeharms, 1997). Stramma and Lutjeharms (1997) have demonstrated that some 20 Sv recirculates in the southwest Indian sub-gyre (Fig.1b). At approximately 90° E, only 20 Sv of the original 60 Sv remains (Stramma and Lutjeharms, 1997). It maybe that the large recirculation in the western half of the South Indian Ocean is connected to bottom topography as about 20 Sv recirculates when crossing the southwest Indian Ridge northwest of the Crozet Islands (46° S, 50° E), whilst the other 20 Sv recirculates in the Crozet Basin west of the Kerguelen-Amsterdam Passage (70° E) (Stramma and Lutjeharms, 1997). The recirculation within the Southwest Indian sub-gyre flows north to north-westwards across the Madagascar Ridge.

Examination of altimetric data shows that several of the Madagascar Ridge seamounts lie in the area of slow mean westward flow between the southern tip of Madagascar (25 °S) and the Agulhas Return Current (ARC) — flowing eastward between 37 °S and 40 °S (Pollard and Read, 2017). The mean westward drift of mesoscale features was 4.1 cm s^{-1} integrated between Madagascar and 37 °S This westward drift can account for 50 Sv, which added to 25 Sv of southward flow past Madagascar, is sufficient to account for the total Agulhas Current transport of 70 ± 21 Sv . Observations with altimetry data show the Walters Shoal on the southern Madagascar Ridge to be regularly affected by eddies which propagate south-westwards from East of Madagascar. These eddies can be identified by their lower oxygen values relative to the surrounding area (above 50 m), i.e. due to the origin of the water being from the northern region (4.9 ml l^{-1}) which contains STSW (Sub tropical surface water; Pollard and Read, 2017)

1.5 About this Paper

This paper is the first to focus on the oceanography of the Madagascar Ridge. It aims to describe the annual (seasonal) climate (wind field), ocean properties (SST, MLD, Heat flux) and ocean circulation (EKE, currents) in the vicinity of the ridge, and to highlight environmental variation which influences the biology of the region and its connectivity. The ridge occurs in a region that seldom sees scientific investigation especially using research vessels. Consequently, we use satellite observations, but have added a novel technique of deploying 'virtual moorings' along the 1 300 km ridge to better characterise ocean circulation and its variability. This is done using altimetry data. The paper is intended to deliver a greater backdrop to a series of more focused physical and biological studies in a special issue that investigate flow-topographic interactions of a shallow seamount (260 m) on the northern ridge, the Walters Shoal (20 m), and to a lesser extent, a shallow seamount (60 m) near Reunion (La Perouse) (i.e. Collins et al., this issue; Demarcq et al., this issue; Vianello et al., this issue; Koch-Larrouy, this is issue). In addition, two ADCP current profiler moorings were deployed near the Mad-Ridge seamount summit between October 2016 and October 2018 (to be published later).

2. Data and methods

2.1 Bathymetry

The GEBCO 2014 bathymetry product was used to reveal the Madagascar Ridge and seamounts. This comprises a global terrain model for ocean and land at 30 arc-second intervals.

2.2 Virtual Moorings

As shown in Fig 2, seven (numbered 1-7) 'virtual mooring' (VM) points were selected along the Madagascar Ridge to investigate the circulation dynamics along this feature, including the MAD-Ridge seamount (virtual mooring 2) and the Walters Shoal (virtual mooring 6). Depths at each virtual mooring 1 – 7 (north – south) position (GEBCO 2014) are 1820 m (46.25 °E 26.5 °S), 260 m (46.25 °E 27.5 °S), 3170 m (46.25 °E 28.5 °S), 2520 m (45.63 °E 30.38 °S), 1200 m (44 °E 32.25 °S), 18 m (44 °E 33.25 °S) and 2330 m (44 °E 34.25 °S). Altimetry data described below were used to calculate current vectors for each position every five days over a period 1998 – 2016.

2.3 Altimetry data

Merged, daily interpolated, Delayed Time (DT), altimetry data gridded at ¼° resolution were used. This product is produced by Ssalto/Duacs and is distributed by the Copernicus Marine Environment Monitoring Service (CMEMS) (http://marine.copernicus.eu/). Mean Absolute Dynamic Topography (MADT) data are used to highlight the circulation dynamics (using climatologies) over the Madagascar Ridge. Mean Eddy Kinetic Energy (EKE) is derived from the MADT data over a specified domain in the Southwest Indian Ocean that includes the entire Madagascar Ridge. This is calculated using the follow equation:

$$\overline{EKE} = \frac{1}{2}\left(\overline{u_g'^2} + \overline{v_g'^2}\right),$$

where $\bar{.}$ stands for a time average, over the 1998 – 2016 period, $u_g'^2$ and $v_g'^2$ being the zonal and meridional components of the surface total geostrophic current directly computed from the MADT. Mean Absolute Dynamic Topography (MADT) data (total geostrophic velocity) is used for data at 7 virtual mooring points along the Madagascar Ridge for 4 years (2011 – 2014).

2.4 Satellite-tracked surface drifters (SVPs) to validate MADT derived velocity vectors

To gain confidence in the geostrophic vectors calculated from the altimetry data, SVP surface drifters were used in this study. Guidelines by the World Ocean Circulation Experiment (WOCE) standards, minimise downwind slip to < 0.7 cm s^{-1} in 10 m s^{-1} winds (Niiler et al., 1995). The floats have an attached drogue centred at 15 m. Six SVP (Surface Velocity Programme) drifters were released from the South African *RV Algoa* on 27 May 2014 near the Walters Shoal and tracked for 24 days (Fig. 3). The trajectories are compared to the 'virtual track' of a particle released close to the Walters Shoal. The virtual track was determined using altimeter-derived daily flow vectors (progress vector analysis).

It needs to be noted that the MADT data does not include the Ekman Component of the circulation. The OSCAR product (https://www.esr.org/research/oscar/oscar-surface-currents/) however does. This is a direct computation of global surface currents using satellite sea surface height, wind, and temperature. Currents are calculated using a quasi-steady geostrophic model together with an eddy viscosity based wind-driven ageostrophic component and a thermal wind adjustment. The model calculates a surface current averaged over the top 30m of the upper ocean. The OSCAR product should therefore be a more accurate reflection of near surface currents. Interestingly, however, comparisons with the MADT vectors and the SVP drifters, showed the OSCAR product to poorly perform — certainly in the Southwest Indian Ocean region. For this reason, we used the MADT for our study.

2.5 SST, Chlorophyll and wind data

Daily Level 2 MODIS sea surface temperature (SST) and chlorophyll a (Chl-a, mg m^{-3}) data (http://modis.gsfc.nasa.gov/) were downloaded to produce climatologies over the Madagascar Ridge at a spatial resolution of 1 km x 1km.

Wind data obtained from http://www.remss.com/measurements/ccmp/ were used to produce climatologies with a spatial resolution of 0.25° and a temporal resolution of one day. These data representing a measurement 10 m from the surface, are a Cross-Calibrated, Multi-Platform (CCMP), gridded product that uses a combination of radiometer wind speeds, QuikSCAT and ASCAT scatterometer wind vectors, moored buoy and model wind data — and is a Level 3 ocean vector wind analysis product (Atlas et al., 2011).

2.6 Heat Flux and Mixed Layer Depth (MLD)

Heat flux data were obtained from https://eo4society.esa.int/2018/08/22/1992-2017-ocean-heat-flux-time-series/ and to produce climatologies over the Madagascar Ridge with a spatial resolution of 0.25° and a temporal resolution of one day. Mixed layer depth (MLD) data were downloaded from http://www.ifremer.fr/cerweb/deboyer/mld/home.php) and used to produce climatologies with a spatial resolution of 2° with a temporal resolution of one month. The criteria to obtain the MLD was as follows: MLD = depth where ($\theta = \theta_{10m} \pm 0.2$ °C) according to de Boyer Montegut et al. (2004).

2.7 Anomalous Events

Unusual (referred to as anomalous henceforth) events were identified in the 24-year geostrophic velocity record (1993 – 2016). Normalized anomalies were obtained by removing the seasonal signal and applying the following equation:

$\text{N.A.}_{\text{Normalized Anomaly}} = (\text{Total Geostrophic velocity} - \text{Total Geostrophic velocity}_{\text{climatology}}) / \text{Standard Deviation}_{(\text{24 values representing 24 years})}$.

Normalized anomalies greater than one standard deviation were classed as anomalous events

2.8 Velocity distribution

The number of counts for each velocity bin of 2 cm s^{-1} for each mooring between 1993 and 2016 was calculated between 0 and 120 cm s^{-1} (i.e. frequency). Subsequently, the number of counts within 10 cm s^{-1} of the maximum number of velocity counts was calculated for each virtual mooring.

3. Results

3.1 Surface Winds

Figs. 4a and 4b show the summer (a) and winter (b) climatology (1995 – 2016) for the regional wind field inclusive of the Madagascar Ridge (in this study summer refers to December, January and February whilst winter refers to June, July and August). Colours represent wind speed with direction indicated by the white arrows (vectors). The black horizontal lines indicate the latitude of the Mad-Ridge seamount and the Walters Shoal. Fig. 5a compliments Figs. 4a and 4b showing summer and winter winds speeds (m s^{-1}) along the N-S transect on the ridge. In summer (austral) the wind direction is easterly along the entire ridge with a northward gradient of increasing speed to a maximum around 9 m s^{-1}. This is expected as the region is strongly influenced by the tropical easterlies i.e., Trade winds. Note that the wind field not only deflects around southern Madagascar but there is also local acceleration there too. This is further highlighted by Collins et al. (this issue). 'Zero wind stress curl' occurs around 36°S at the southern extreme of the ridge with the Westerly Belt beginning south of this.
In winter the zero wind stress curl moves northwards to beyond the Walters Shoal (32°S) along with northward migration of the westerly wind belt (Rubin et al., 1953) — the latter encroaching the southern part of the ridge. As seen in Fig. 5a winds speeds in winter become very strong over the southern ridge reaching averages maximums of around 11 m s^{-1}. The local wind acceleration south of Madagascar appears to be an annual feature.

3.2 Sea Surface Temperature (SST)

Figs. 4c and 4d depict the regional SST climatology (1998 – 2014) with Fig 5c similarly showing SST along the N-S transect. A strong gradient is observed in both seasons increasing during summer from 17°C at 40°S to about 26°C near Madagascar, and in winter 16°C to 24°C respectively. Specifically at the Walters Shoal, the SST ranges from 22 ± 0.7°C in summer to 19 +-0.4 °C in winter. In contrast, the MAD-ridge seamount has a summer climatology of 26 ± 0.4C whilst in winter this drops to 23 ± 0.5 °C. Both seamounts have approximately the same difference in SST (climatology) between summer and winter.

It should be noted that the Walter Shoal is in a region where STSW (Sub-Tropical Surface Water) is predominant in the surface layers (Read and Pollard., 2017), whilst the MAD-ridge seamount is in a region where TSW (Tropical Surface Water) is predominant in the surface layers (Vianello et al, this issue). STSW is saltier than TSW (STSW has salinity values > 35.5 and a temperature range of 17 °C – 20 °C whilst TSW has salinity values < 35.5 and temperature values > 24° C (Pollard and Read, 2017; Swallow, J.C et al, 1988)). Although it must be noted that during the summer the surface climatology around the Walters shoal is > 20 °C (22 °C). The likely cause is due to air-sea interaction. The climatology subsurface is likely within the STSW range of 17 °C – 20 °C (Read and Pollard., 2017).

3.3 Mixed layer depth (MLD)

Figs 4e and 4f show the MLD climatology (1995 – 2016) over the region, similarly with Fig 5f the along ridge gradient. Note the colour scale differs. During summer (Fig. 6e) the MLD varies little (± 2 m) along the Madagascar Ridge. For example, the MLD at 30°S; 47°E is 23.73 m ± 4.25 m. To the west of the ridge (30°S; 40°E) in the Mozambique Basin, it is 29.78 m ± 5.38 m. To the east of the ridge on the same latitude (30°S; 51°E) the MLD is 24.03 ± 4.16 m.

During winter however, greater contrasts exist in the region between the north and south ranging from nearly 120 m at 40°S to 58 m near the MAD-Ridge seamount — the former strongly tied to the northward creep of the westerly wind belt. For example, at 26°S; 47°E the MLD is 58.04 ± 16.7 m, at 30°S; 47°E the MLD is 64.76 ± 13.89 m, whilst at 34°S; 47°E the MLD is 99.88 ± 22.51 m. Additionally, the MLD varies longitudinally (west of the Madagascar ridge to the east). The MLD to the west of the ridge (30°S; 40°E) is 62.86 ± 15.65 m, whilst to the east of the ridge (30°S; 51°E) MLD values are 68.6 ± 9.29 m. There is some deepening of the MLD to the west of southern Madagascar.

3.4 Surface Heat Flux

As seen in Figs 4g and 4h, and Fig. 5e — the heat flux climatology (1985 – 2016) varies both latitudinally across the Madagascar Ridge and between seasons. Positive values indicate a downward flux. During summer there is a positive heat flux over the ridge but this changes in winter to negative (Note the colour scales are not the same). A maxima is found in the vicinity of 35 °S (summer) and 32.5 °S (winter). Table 1 indicates that the heat flux increases (decreases) southward across the ridge during the summer (winter) but reverses south of the Madagascar Ridge. However, as seen by the standard deviations, the heat flux is highly variable over the ridge.

3.5 Eddy Kinetic Energy (EKE)

As depicted in Figs. 4i and 4j which show the EKE climatology (1993 – 2016), there is very little difference between the summer and winter regimes over the Madagascar Ridge. But as starkly seen in Fig. 5b, the northern part of the Madagascar ridge lies in a zone of high eddy activity. In contrast, the southern part of the Madagascar ridge lies in a zone of low eddy activity. Towards 40°S the EKE increases due to eddy activity on the northern boundary of the STC. This means the MADRidge seamount and Walter Shoal are positioned in completely different EKE regimes. During both summer and winter the EKE near the Walter Shoal has an EKE climatology of < 50 cm^2s^{-2} whilst the MAD-Ridge seamount is approximately 400 cm^2s^{-2}. The literature sclimatology smooths out eddies near the Walters Shoal as literature suggests (Pollard and Read, 2017). The Walters Shoal lies in a quiescent zone between the EMC (and the EMRC) to the north and the ARC (Agulhas Return Current) to the south.

3.6 Surface Chlorophyll (Chl-a)

Figs 4k and 4l show the surface summer and winter Chl-a climatology (1998 – 2015) respectively, with Fig 5d highlighting the along-ridge gradients. Summer experiences low values of approximately 0.1 mg m^{-3} over much of the ridge except for the extreme northern and southern areas — the former being on the Madagascar shelf. The MADRidge seamount has a summer mean of 0.14 ± 0.03 mg m^{-3} with the Walters Shoal 0.14 ± 0.03 mg m^{-3}. Due to wind-induced vertical mixing (Fig 5f; Martin and Shaji., 2015) levels of Chl-a increase during winter along the entire ridge except for the Madagascan shelf which shows a contrasting summer-winter regime (Collins et al., this issue). The mean over the Walters Shoal is 0.26 ± 0.04 mg m^3 and the MADRidge seamount 0.19 ± 0.02 mg m^{-3}.

3.7 General ocean circulation in the region

Fig. 6 shows the summer and winter climatologies (1993 – 2016) of the circulation in the vicinity of the Madagascar Ridge. Eddies — especially dominant over the northern Madagascar ridge (Vianello et al., this issue; Halo et al., 2014) — are smoothed out in the climatology. As expected, the major high velocity currents i.e., the EMC, Agulhas Current and the ARC, are conspicuous all-year round with little seasonality in position and speed, with the exception of the EMC is on average stronger in winter than summer (i.e., 60 vs 70 cm s^{-1}). As clearly seen, the northern part of the ridge is dominated by the EMC that empties into the Mozambique Basin with continued transport towards the Agulhas Current, and to the east into the SICC through the retroflection. The powerful ARC does not impact the ridge, but rather flows over the Southwest Indian Ridge much farther south. Currents over the central and southern parts (i.e. most of the ridge) of the ridge indicate on average low velocities (15 cm s^{-1}) with a north-westward mean direction.

3.8 Geostrophic current field over the Ridge (Virtual Moorings)

The geostrophic currents across the Madagascar Ridge are shown in Fig. 7 as 4-day, vector time series plots for the years 2011 – 2014 for each of the 7 virtual mooring (VM) points. As clearly seen geostrophic velocities generally decrease from north to south with the EMC (constant south-westerly direction) strikingly visible at VM 1 whilst the lowest velocities occur at VM 6 (Walters Shoal). There is no consistent direction in the geostrophic velocities at the other six virtual mooring positions.

The geostrophic velocities north of the MAD-Ridge seamount at VM 1 are dominated by the south-westward flowing EMC. Velocities within the EMC are generally 50 – 60 cm s^{-1} but can reach up to 100 cm s^{-1} (e.g. 27 November 2014). This is with the very dynamic region where the EMC terminates (Figs 1a and 6). Geostrophic velocities at the MAD-Ridge seamount, VM 2 are generally lower than VM 1. Here velocities range between 30 - 40 cm s^{-1}. However, whilst velocities can reach up to 100 cm s^{-1}, the direction of the currents are not as constant as at VM 1. The MAD-Ridge seamount is also in a zone of high eddy activity with mesoscale eddy activity (Fig 4) occurring 93.8% of the time (1993 – 2016) (Vianello et al., this issue). The current direction difference at VM 2 is primarily due to the presence of mesoscale eddies (either polarity) but also due to the south-westward flowing EMC and the north-eastward flowing EMRC.

The velocities at VM 3 have a similar range as VM 2 (i.e. 30 – 40 cm s^{-1}) and there is little coherency in the direction of the currents here. Interestingly, currents can reach up to 100 cm s^{-1}, although not as often as VM 1 in the direct path of the EMC) (Fig. 6). The change in direction of the currents are due to mesoscale eddies and the EMRC (too far south for the passage of the EMC). Geostrophic velocities at VM 4 generally have geostrophic velocities in the range of 20 – 30 cm s^{-1} but can reach up to 50 cm s^{-1}. The primary reason for increased velocities in the region is due to transient westward moving eddies (Quartly et al., 2006). Velocities are rarely near the Walters Shoal. VM 5 and 6 generally being around 10 cm s^{-1}. However, on occasion transient westward moving eddies can cause velocities to reach 55 cm s^{-1} at VM 5 (i.e. 10 February 2012). There is a slight increase in the magnitude of geostrophic velocities at VM 7 ranging between 10 – 20 cm s^{-1}.

Fig. 8 shows the velocity statistics at the seven VMs along the Madagascar ridge from 1993 - 2016. Generally, the highest number of counts of velocity magnitude for each mooring decreases with increasing latitude except for VM 6 (Walters Shoal) where the highest number of counts (293 counts) is higher than VM 7 (211 counts) and higher than any other virtual mooring. Additionally, the velocity range decreases with increasing latitude (VM 1 has the highest velocity range). This decreasing range is depicted in Table 1 where the velocity magnitude counts within 10 cm s^{-1} of magnitude of velocity with highest number of counts increases with latitude. The virtual moorings towards the southern part of the Madagascar ridge (VM5, VM6, VM7) has more counts of velocity within 10 cm s^{-1} of the magnitude of velocity with the highest number of counts (> 80%) than towards the northern part of the Madagascar ridge (VM1, VM2, VM3) (< 50%).

Tables 2 and 3 show the statistics of the direction of the currents for the seven virtual moorings down the Madagascar Ridge during the period 1993 – 2016. Five of the seven virtual moorings exhibited a double maxima in the direction counts. Virtual mooring one exhibits the direction of maximum counts to be 245° (South-Westerly) and the count is 1227 (71.06%). This relatively high number indicates that virtual mooring one lies in a zone of relatively constant velocity direction which is an indication of the EMC (East Madagascar Current). The other six virtual moorings indicate varying directions of current velocity.

3.9 Geostrophic Velocity Climatologies

Fig. 9 sums up these results and shows the monthly climatology of geostrophic currents (1993 – 2016) across the Madagascar ridge. The EMC (centred at 26.5 °S) has near constant values throughout the year of 60 - 70 cm s^{-1} in a south-westerly direction. The EMRC which is centred at 28° S displays seasonality in both magnitude and direction. During the austral summer velocities are in a north-easterly direction with values of 15 – 25 cm s^{-1} whilst during the austral winter velocities are in a north-north-easterly direction with values of 8 – 10 cm s^{-1} with the exception of August where velocities are in an easterly direction with the same magnitude. The MAD-Ridge seamount has low velocities throughout the year (between 7 – 15 cm s^{-1}). The Walters Shoal exhibits minimal velocities throughout the year (< 5 cm s^{-1}). Of interest is the current climatology at the southernmost virtual mooring - 7 (34.25 °S). During the austral summer, velocities are in a north-easterly direction with magnitudes of 15 cm s^{-1}. During the austral winter, velocities are negligible (< 5 cm s^{-1}).

3.10 Anomalous events in the velocity field over the northern Madagascar Ridge

Three events over the time span 2011 to 2014 are highlighted in the geostrophic velocity field over the Madagascar Ridge — (a) 15 January 2012 (Normalized Anomaly – 2.1 – VM 5; Fig. 10a), (b) 30 December 2012 (Normalized Anomaly – 1.7 – VM 4; Fig. 10b) and (c) 27 September 2014 (Normalized Anomaly – 1.6 – VM 1; Fig. 10c). These show that the northern ridge can have some complex flow configurations and these vary significantly, which most probably have varying implications for the local biology. In the case of (a), the striking feature in the horizontal velocity field is a tight retroflection of the EMC at 28 °S 44 °E with what seems to be a large anticyclone immediately to the south. This extends southwards to 32° E mid-way along the ridge. The EMRC/SICC flows beyond 55° E. Velocities at mooring 5 are 62 cm s^{-1} (easterly). Farther north the velocity is lower (10 cm s^{-1}) at mooring 4 which borders the eddy center. Depression of the thermocline in the anticyclonic center will most likely not promote productivity over the ridge.

In the case of (b), the velocity field indicates intense eddies to the west of the ridge and similarly with a tight EMC retroflection. The EMC flows across VM 1 with velocities of 67 cm s^{-1} whilst the EMRC drifts southward towards VM 4 with velocities of 49 cm s^{-1} before drifting north-eastward and meandering eastward past the east coast of Madagascar. To the south velocities drop off. At VM 5 the velocity is 17 cm s^{-1} with a north- eastward direction whilst the velocity at VM 6 has a westward direction (Walters Shoal) with a magnitude of 8 cm s^{-1}. Velocities at VM 7 are 11 cm s^{-1} in a north-westerly direction. A clockwise eddy is observed just north of the ARC (41 °E 37 °S). In the case of September 2014 (c), there is an early retroflection of the EMC (26.5° S 47.5 °E). This is indicated by below average velocities at VM 1 and 2 (11 cm s^{-1} and 17 cm s^{-1}, respectively). There is a north-westward current from the ARC region (36 °S 57.5 °E) towards VM 4 where velocities are 35 cm s^{-1}.

Discussion

The Madagascar Ridge has a distinct lack of in-situ observations. In this study we provide the first description of surface winds, SST, MLD, EKE, Surface Heat Flux and Chl-a in the vicinity of this feature. The novel approach of deploying virtual moorings has greatly helped us gain a better understanding of the circulation in the Southwest Indian sub-gyre, and moreover, the circulation in the greater region which acts as a source for the strong western boundary Agulhas Current (Stramma and Lutjeharms., 1997). We produced a 4-year time series of geostrophic velocities between 2011 and 2014 at seven positions along the Ridge spanning 10 degrees of latitude. The geostrophic vectors obtained using MADT data are reliable since good correlations were found with in-situ SVP drifters. It should however be noted that the geostrophic velocities obtained from the altimetry are a little lower than the drifter velocities due to tempo spatial resolution, and do not take Ekman transport into account.

The results provide a backdrop to other more focussed physical and biological oceanographic studies of three seamounts undertaken during the MADRidge project and published in this Special Issue — two of which lie on the Madagascar Ridge (i.e. Mad-Ridge seamount and Walters Shoal). We have broadly described the wind field over the Madagascar Ridge identifying a localised 'hotspot' of accelerated wind speed off the SE coast of Madagascar that exists during both summer and winter with speeds slightly stronger during the winter. This possibly plays a role in the localized upwelling found there and therefore high productivity (Collins et al., this issue). The EKE differs vastly between the northern section of the ridge (where the Mad-Ridge seamount is located) and the southern section of the ridge where the Walters Shoal is located, and hence there is a vast difference in the current regime with higher currents over the northern section. This has a potential impact on the retention/dispersion of nutrients and larvae over the Mad-Ridge and Walters Shoal as highlighted in a connectivity study based on IBM modelling (Crochelet et al., this issue). Additionally, the productivity over the two seamounts (depicted by the surface signature of Chl-a used as a proxy of phytoplankton biomass; Demarcq et al., this issue) may be affected by the observed current regimes by preventing Chl-a retention — by preventing the formation of Taylor Columns (Vianello et al., this issue).

The MLD across the Madagascar Ridge potentially has an effect on zooplankton communities (zooplankton abundance and biovolume) and is analysed over the two shallow seamounts on the Madagascar Ridge (Mad-Ridge seamount and the Walters Shoal) (Noyon et al., this issue). This will in turn affect the composition and abundance of species higher up the food chain such as fish larvae (Harris et al., this issue). It must be noted that the connectivity (fish larvae) between nearby shelves to the seamounts are likely affected by the currents in the region as (Vianello et al., this issue) established that dipoles/eddies draw Chl-a off the Madagascar shelf towards the Mad-Ridge seamount. To further support this conclusion (Harris et al., this issue) found similar fish larvae species over the Mad-Ridge seamount to that over the Madagascar shelf. It is important to note that the ocean circulation over the northern Madagascar Ridge is highly dynamic and has the potential to substantially affect the biology in the region. For instance, the EMC, EMRC and its retroflection is not a permanent feature south of Madagascar with respect to its presence and position as on many occasions are replaced by mesoscale eddies and dipoles (Vianello et al., this issue). During the research cruise on the R/V Antea between 8 November 2016 – 13 December 2016 a relatively strong dipole was observed over the Mad-Ridge seamount. However, the EMC was still present off the SE coast of Madagascar. Such events in combination with events such as the existence of relatively low currents for the region over the Mad-Ridge seamount (27 September 2014) when there was an early retroflection (the EMC was present off the east coast of Madagascar but not off the southeast and south coast) may have a dramatic effect on the ecology over the Mad-Ridge seamount. Further research cruises and deployment of moorings during periods of different ocean circulation patterns are required for further studies into the effect of the Mad-Ridge on the ecology in the region of the seamount. Furthermore, during more quiescent conditions, there may be an enhanced effect of current-topography interactions over the Mad-Ridge seamount such as the formation of Taylor Columns as it has been theoretically proven that they can exist over the Mad-Ridge seamount (Vianello et al., this issue). The dynamics of the area however probably wouldn't permit an ecosystem response. On the other hand, weak currents would be more compatible with TC influence on ecosystems at the Walters Shoal but with a limited spatial extension as the seamount is very shallow.

Our results also show that, while almost no seasonality occurs in the current dynamics across the Madagascar Ridge (Fig. 4), other parameters important for ecosystems functioning such as sea surface Chl-a, mixed layer depth, heat fluxes, and wind speeds show significant variability throughout year and all along the Ridge (Fig. 6). This might have important consequences in terms of biological productivity as well as on the success of larval transport to consider in connectivity studies (i.e. Crochelet et al. this issue).

Acknowledgements

The MADRidge project formed a constituent of the IIOE2 Western Indian Ocean Upwelling Research Initiative (WIOURI) — specifically RUP 3 (Roberts., 2015). It was a joint venture between the IRD (France) and the Nelson Mandela University in South Africa, with support from the UK Newton Fund and National Research Foundation (NRF) in the form of Prof Roberts' UK-SA Bilateral Research Chair.

References

Atlas, R., Hoffman, R., Ardizzone, J., Leidner, S., Jusem, J., Smith, D., Gombos, D., 2011. A cross-calibrated, multiplatform ocean surface wind velocity product for meteorological and oceanographic applications. Bull. Amer. Meteor. Soc., 92, 157-174.

Beal, L., Bryden, H., 1999. The velocity and vorticity structure of the Agulhas Current at 32° S. J. Geophys. Res. Oceans 104(C3), 5151 - 5176.

Belkin, I., Gordon, A., 1996. Southern Ocean fronts from the Greenwich meridian to Tasmania. J. Geophys. Res. Oceans 101(C2), 3675 - 3696.

Boebel, O., Rossby, T., Lutjeharms, J.R.E., Zenk, W., Barron, C., 2003. Path and variability of the Agulhas Return Current. Deep Sea Res. II 50(1), 35 – 56

Bryden, H., Longworth, H., Cunningham, S., 2005. Slowing of the Atlantic meridional overturning circulation at 25° N. Nature 438, 655 – 657.

Buijsman, M., Ansong, J., Arbic, B., Richman, J., Shriver, J., Timko, P., Wallcraft, A., Whalen, C., Zhao, Z., 2016. Impact of Parameterized Internal Wave Drag on the Semidiurnal Energy Balance in a Global Ocean Circulation Model.. J. Phys. Oceanogr. 46, 1399 - 1419.

Chelton, D., Schlax, G., Samelson, M., 2011. Global observations of nonlinear mesoscale eddies. Prog. In Oceanogr. 91(2), 167 - 216.

Collins M., Ternon J.-F., Demarcq H., Herbette S., Roberts M., this issue. An upwelling cell off the

southeast coast of Madagascar.

Crochelet, E., Barrier, N., Andrello, M., Marsac, F., Spadone, A., Lett, C., this issue. Connectivity between seamounts and coastal ecosystems in the South West Indian Ocean.

de Ruijter, W., Ridderinkhof, H., Schouten, M., 2005. Variability of the southwest Indian Ocean. Philos. Trans. Roy. Soc. A: Math., Phys. and Eng Sci. 363(1826).

Da Silva, J., New., A., Magalhaes., 2009. Internal solitary waves in the Mozambique Channel: Observations and interpretation. J. Geophys. Res. Oceans 114(C5).

Demarcq H., Roberts M., Noyon M., this issue. Enhanced planktonic biomass associated with seamounts and islands in the south-western Indian ocean from ocean colour data.

De Boyer Montegut, C., Madec, G., Fischer, A., Lazar, A., Iudicone, D., 2004. Mixed layer depth over the global ocean: An examination of profile data and a profile-based climatology. J. Geophys. Res. 109(C12003).

de Ruijter, W., van Aken, H., Beier, E., Lutjejarms, J.R.E., Matano, R., Schouten, W., 2004. Eddies and dipoles around South Madagascar: formation, pathways and large-scale impact. Deep Sea Res. I 51(3), 383 – 400.

Goslin, J., Segoufin J., Schlich, R., Fisher, R., 1980. Submarine topography and shallow structure of the Madagascar Ridge, western Indian Ocean. GSA Bull. 91(12).

Talley, L.D., Pickard, G.L., Emery, W.J., Swift, J.H., 2011. Descriptive Physical 948 Oceanography, sixth ed. Academic Press.

Halo, I., Penven, P., Backeberg, B., Ansorge, I., Shillington, F., Roman, R., 2014. Mesoscale eddy variability in the southern extension of the East Madagascar Current: Seasonal cycle, energy conversion terms, and eddy mean properties. J. Geophys. Res. Oceans 119(10), 7324 - 7356.

Harris, S., Noyon, M., Roberts, M., Marsac, F., this issue. Ichthyoplankton assemblages at three shallow seamounts in the South West Indian Ocean: La Pérouse, MAD-Ridge and Walters Shoal.

Kanaev, V., Smilsova, N., 1975. Bottom topography of the Indian Ocean. In: Geological-Geophysical Atlas of the Indian Ocean, Udinstev, G., ed. Moscow, Academy of Sciences of the USSR.

Killworth, P., Chelton, D., De Szoeke, R., 1997. The Speed of Observed and Theoretical Long Extratropical Planetary Waves. J. Phys. Oceanogr. 27, 1946 – 1966.

Koch-Larrouy A., Ternon, J.-F., Roberts, M., Herbette. S., Arbic, B., Chanut, J., Lyard, F., Bourdalle-Bady, R., Ansong, J., Tchilibou, M., Buijsman, M., Vianello, P., Allain, D., Demarcq, H., Shriver, J., Ferron, B., this issue. Mixing above a group of seamounts on the northern Madagascar Ridge with impacts on algal blooms.

Lutjeharms, J.R.E., 1988. Remote sensing corroboration of retroflection of the East Madagascar Current. Deep Sea Res. A 35(12), 2045 – 2050.

Lutjeharms, J.R.E., 2007. Three decades of research on the greater Agulhas Current. O. Sci. Europ. Geosci. Un. 3 (1), 129-147.

Lutjeharms, J.R.E., Ansorge, I., 2001. The Agulhas Return Current. J. Mar. Sys. 30(1-2), 115 – 138.

Lutjeharms, J.R.E., Bang, N., Duncan, C., 1981. Characteristics of the currents east and south of Madagascar. Deep Sea Res. A 28(9), 879 – 899.

Lutjeharms, J.R.E., Machu, E., 2000. An upwelling cell inshore of the East Madagascar Current. Deep Sea Res. I 47(12), 2405 – 2411.

Martin, M., Shaji, C., 2015. On the eastward shift of winter surface chlorophyll-a bloom peak in the Bay of Bengal. J. Geophys. Res. Oceans 120, 2193 - 2211.

Morgan, W., 1972. Deep mantle convection plumes and plate motions. AAPG Bull. 56(2), 203 – 213.

Nauw, J., van Aken, H., Webb, A., Lutjeharms, J.R.E., de Ruijter, W., 2008. Observations of the southern East Madagascar Current and undercurrent and countercurrent system. J. Geophys. Res. 113(C08006).

Niiler, P., Sybrandy, A., Kenong, B., Poulain, P., Bitterman, D., 1995. Measurements of the water-following capability of holey-sock and TRISTAR drifters. Deep-Sea Res. I 42, 1951 – 1964.

Parin, N.V., Nesis, K.N., Sagaidachny, A.Y., Shcherbachev, Y.N. 1993. Fauna of Walters Shoal, a seamount in the southwestern Indian Ocean. Trudy Institut. Okanologii. 128, 199-216

Palastanga, V., van Leeuwen, P., Schouten, M., de Ruijter, W., 2007. Flow structure and variability in the subtropical Indian Ocean: Instability of the South Indian Ocean Countercurrent. J. Geophys. Res. Oceans 112(C1).

Pinet, P., Jaquemet, S., Phillips, R.A., Le Corre, M., 2012. Sex specific foraging strategy throughout the breeding season in a tropical, sexually monomorphic small petrel. Animal Behaviour, doi:/10.1012/j.anbehav.2012.01.19

Pollard, R., Read, J., 2017. Circulation, stratification and seamounts in the Southwest Indian Ocean. Deep Sea Res. II 136, 36 - 43.

Quartly, G., Buck, J., Srokosz, M., Coward, C., 2006. Eddies around Madagascar — The retroflection re-considered. J. Mar. Sys. 63(3-4), 115 - 129.

Quartly, G., Srokosz, M., 2004. Eddies in the southern Mozambique Channel. Deep Sea Res. II 51(1-3), 69 – 83.

Ramanantsoa, J., Krug, M., Penven, P., Rouault, M., 2017. Coastal upwelling south of Madagascar: Temporal and spatial variability. J. Mar. Sys. 178, 29 – 37.

Read, J., Pollard, R., 1993. Structure and transport of the Antarctic Circumpolar Current and Agulhas Return Current at 40°E. J. Geophys. Res. Oceans 98(C7), 12281 - 12295.

Read, J., Pollard, R., 2017. An introduction to the physical oceanography of six seamounts in the southwest Indian Ocean. Deep Sea Res. II 136, 44 – 58.

Ridderinkhof, W., Le Bars, D., von der Heydt, A., de Ruijter, W., 2013. Geophys. Res. Lett. 40, 558 – 562.

Roberts M., 2015. The Western Indian Ocean Upwelling Research Initiative (WIOURI): A Flagship IIOE2 Project. CLIVAR Exchanges No. 68, Vol. 19, No. 3, Nov 2015

Roberts M., Ternon J.-F., Marsac F., Noyon M., this issue. The MADRidge Project: Bio-Physical coupling around a shallow seamount on the northern Madagascar Ridge, Southwest Indian Ocean.

Rubin, M., van Loon, H., 1953. Aspects of the circulation of the southern hemisphere. J. Met. 11, 68 – 76.

Sangra, P., Basterretxea, G., Pelegri, J., Aristegui, J., 2001. Chlorophyll increase due to internal waves on the shelf break of Gran Canaria (Canary Islands). Sci. Mar. 65, 89-97.

Schouten, M., de Ruitjer, W., van Leeuwen, P.J., Dijkstra, H., 2002. An oceanic teleconnection between the equatorial and southern Indian Ocean. Geophys. Res. Lett. 29(16).

Siedler, G., Rouault, M., Biastoch, A., Backeberg, B., Reason, C., Lutjeharms, J.R.E., 2009. Modes of the southern extension of the East Madagascar Current. J. Geophys. Res. 114(C01005).

Siedler, G., Rouault, M., Lutjeharms, J.R.E., 2006. Structure and origin of the subtropical South Indian Ocean Countercurrent. Geophys. Res. Lett. 33(24).

Somavilla, R., Gonzalez-Pola, C., Fernandex-Diaz, J., 2017. The warmer the ocean surface, the shallower the mixed layer. How much of this is true? J. Geophys. Res. Oceans 122(9), 7698 – 7716.

Stramma, L., Lutjeharms, J.R.E., 1997. The flow field of the subtropical gyre of the South Indian Ocean. J. Geophys. Res. 102(C3), 5513 – 5530.

Swallow, J., Pollard, R., 1988. Flow of bottom water through the Madagascar Basin. Deep Sea Res. A 35(8), 1437 - 1440.

Toole, J., Warren, B., 1993. A hydrographic section across the subtropical South Indian Ocean. Deep Sea Res. I 40(10), 1973 – 2019.

Sybrandy, A., Niiler, P., 1992. WOCE/TOGA Lagrangian Drifter Construction Manual. WOCE Report 63, SIO Reference 91/6. Scripps Institute of Oceanography, La Jolla, CA, 58 pp.

Vianello, P., Ternon, J., Herbette, S., Roberts, M., this issue. Circulation and hydrography in the vicinity of a shallow seamount on the northern Madagascar Ridge.

TABLES

Virtual Mooring (VM)	Summer Heat Flux (W m^{-2})	Winter Heat Flux (W m^{-2})
2 (Northern Madagascar Ridge – Mad-Ridge Seamount)	40.9 ± 45.3	-131 ± 44.7
4 (Central Madagascar Ridge)	58.1 ± 47.7	-79.9 ± 43.3
6 (Southern Madagascar Ridge – Walters Shoal)	88.2 ± 37.5	-77.6 ± 46.4

Table 1. Surface Heat Flux over the Madagascar Ridge

Table 2. Number (and percentage of total) of velocity magnitude counts within 10 cm s^{-1} of magnitude of velocity with highest number of counts

Virtual Mooring	Velocity count	Percent	Magnitude of velocity at highest number of counts (cm s^{-1})
1	554	32.06	51
2	687	39.76	33
3	739	42.77	17
4	1006	58.22	15
5	1452	84.03	11
6	1614	93.4	7
7	1507	87.21	11

Table 3. Number (and percentage of total) of direction counts within 20° of direction with highest number of counts

Virtual mooring	Direction(s) of maximum counts (North = 0°)	Direction count(s)	Percent(s)
1	245	1227	71.06
2	65 \\ 335	452 \\ 284	26.16 \\ 16.44
3	65 \\ 325	437 \\ 179	25.29 \\ 10.36
4	215	324	18.75
5	105 \\ 355	251 \\ 196	14.53 \\ 11.4
6	35 \\ 295	249 \\ 347	14.41 \\ 20.14
7	115 \\ 315	349 \\ 300	20.25 \\ 17.36

Figure Legends

Fig1. (a) Major oceanographic features of the Southwest Indian Ocean.Shaded bathymetry south of Madagascar highlights the Madagascar Ridge.(b) shows the calculated baroclinic volume flux field for the South Indian Ocean over the upper 1000m. Transport volumes are in 10^6 m^3 s^1. Note the intensified flow south of Madagascar referred to as the South Western Indian Ocean sub gyre.This traverses the Madagascar Ridge. Other than this and the dynamics of the East Madagascar Current(EMC),nothing is known of the circulation of the ridge.

Fig2. (a) Bathymetry of the Madagascar Ridge (Gebco2014) with two longitudinal transects.Blockdots (7of them) indicate the position of the virtual moorings referred to in the text.(b) Shows the cross sections of the bathymetry along these transects.Black line in (b)is along the pink transect.Grey shading is along the black 'mooringline'.'x' in (b) depicts the positions of the virtual moorings.

Fig.3. Validation of satellite derived geostrophic currents near Walters Shoal using 6 SVP drifters (coloured tracks) and a geostrophic-derived progressive vector plot (black dots). The tracks are for 24 days.The geostrophic progressive vector (virtual) trajectory follows the tracks of the actual SVP drifters very well but travel s a smaller distance.

Fig.4. Summer and winter wind field and ocean properties in the greater region of the Madagascar Ridge: (a)and (b) Surface winds, (c) and (d)SST, (e) and (f) Mixed Layer Depth, (g)and (h) Total Heat Flux, (i) and(j) EKE, (k) and (l) Chl-a. The two horizontal black lines indicate the latitudes of the MAD-Ridge pinnacle (27.5°S) and the Walters Shoal (33.25°S) whilst the black diamonds indicate the 7 virtual moorings along the Madagascar Ridge. All maps have GEBCO2014 bathymetry overlay.

Fig.4. (Cont.) Summer and winter wind field and ocean properties in the greater region of the Madagascar Ridge:(a) and (b) Surface winds, (c) and (d) SST, (e) and (f) Mixed Layer Depth, (g) and (h) Total Heat Flux, (i) and (j) EKE, (k) and (l) Chl-a. The two horizontal black lines indicate the latitudes of the MAD-Ridge pinnacle (27.5°S) and the Walters Shoal (33.25°S) whilst the black diamonds indicate the 7 virtual moorings along the Madagascar Ridge. All maps have GEBCO2014 bathymetry overlay.

Fig.5. Plots detailing summer (blackline) and winter (blueline) gradients along the center of the Madagascar Ridge:(a)Surface winds, (b)EKE,(c) SST,(d)Chl-a, Total Heat Flux, (f) Mixed Layer Depth.

Fig. 6. Climatology of the circulation in the vicinity of the Madagascar Ridge □□(a) Summer, (b) Winter. GEBCO2014 bathymetry overlay is depicted in white.

Fig.7. Four day time series of geostrophic currents between 2011 and 2014 for the 7 virtual mooring sites (numbered) along the Madagascar Ridge shown on Fig.2.Black horizontal lines depict dates selected for anomalies for the specific mooring.Geostrophic velocities generally decrease from north to south with the EMC(south-westerly direction) clearlyvisible at virtual mooring 1.

Fig. 8. Number distribution of geostrophic velocity magnitude (surface) for virtual moorings 1 -7

Fig.9. Monthly mean climatology of currents across the Madagascar Ridge for the period 1993-2016. The two blue lines indicate the position of theMAD-Ridge pinnacle (27.5°S) and the Walters Shoal (33.25°S) whilst the black line indicates a of change of scale for current strengths indicated (right side of the diagram).

Fig.10. Maps of horizontal geostrophic velocities highlighting anomalous events. (a) 15 January 2012, (b) 30 December 2012, (c) 27 September 2014. (a) indicates the retroflection occurring around VM5, (b) indicates the retroflection occurring around VM4 whilst (c) indicates an early retroflection at near the SE coast of Madagascar and VMs1–3 experience lower than average geostrophic velocities. All maps have GEBCO2014 bathymetry overlay.

(a)

(b)

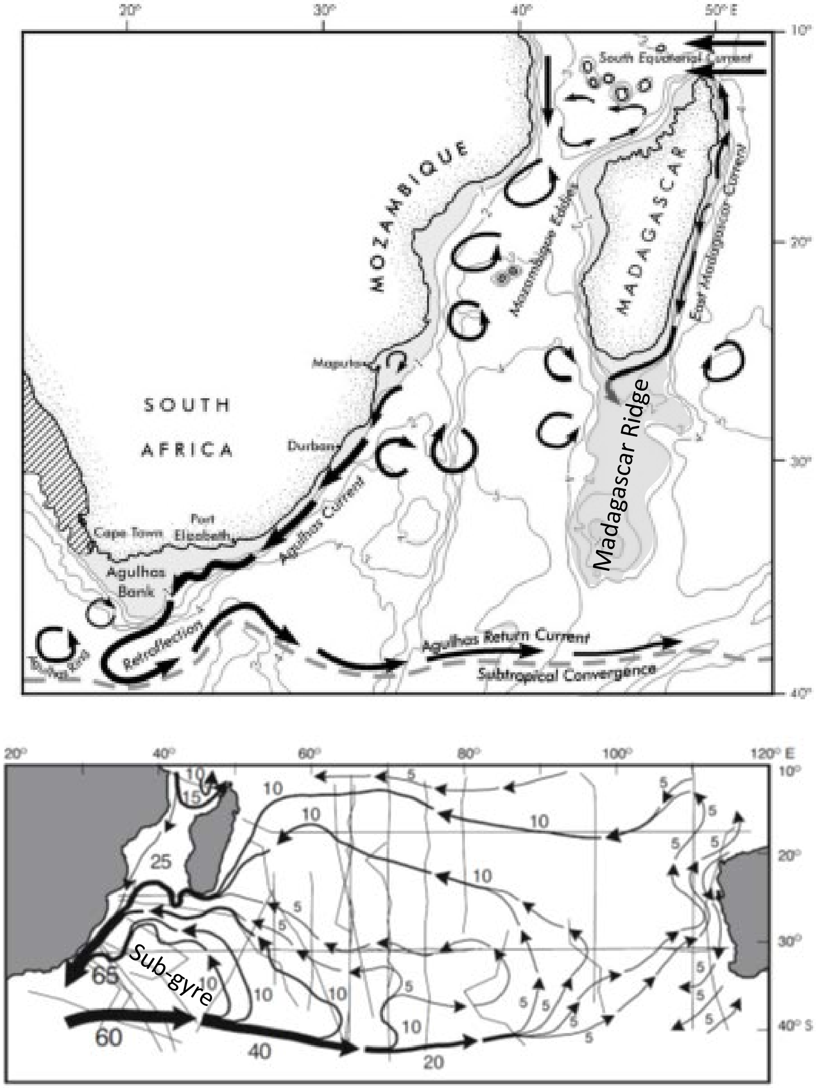

Fig 1. (a) Major oceanographic features of the Southwest Indian Ocean. Shaded bathymetry south of Madagascar highlights the Madagascar Ridge. (b) shows the calculated baroclinic volume flux field for the South Indian Ocean over the upper 1000 m. Transport volumes are in 10^6 m^3 s^{-1}. Note the intensified flow south of Madagascar referred to as the South Wester Indian Ocean sub-gyre. This traverses the Madagascar Ridge. Other than this, and the dynamics of the East Madagascar Current (EMC), nothing is known of the circulation of the ridge.

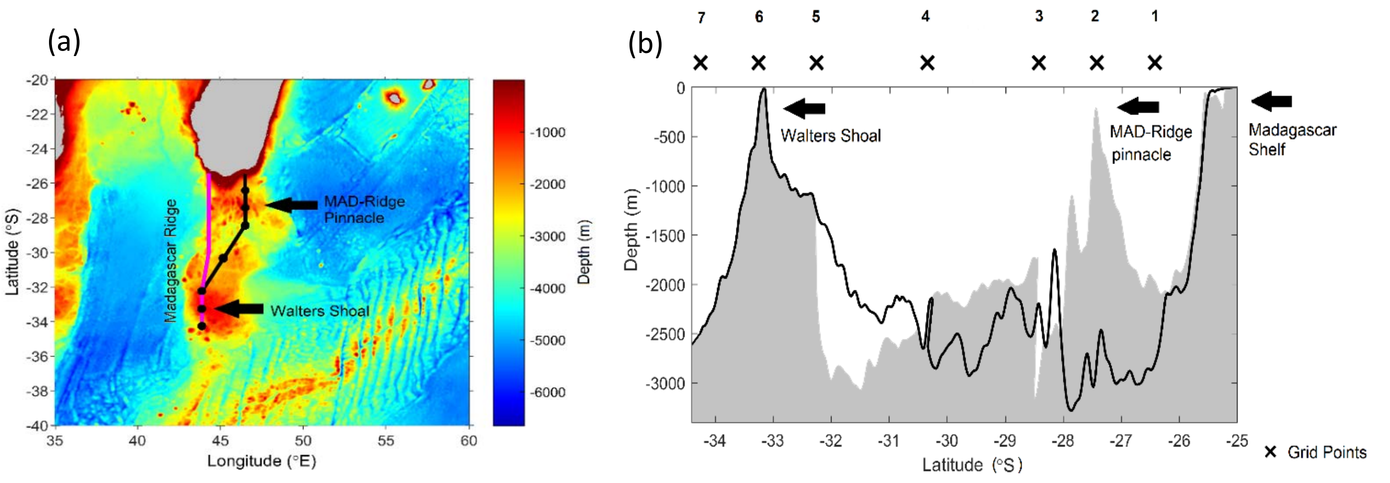

Fig 2. (a) Bathymetry of the Madagascar Ridge (Gebco 2014) with two longitudinal transects. Block dots (7 of them) indicate the position of the virtual moorings referred to in the text. (b) Shows the cross sections of the bathymetry along these transects. Black line in (b) is along the pink transect. Grey shading is along the black 'mooring line'. 'x' in (b) depicts the positions of the virtual moorings.

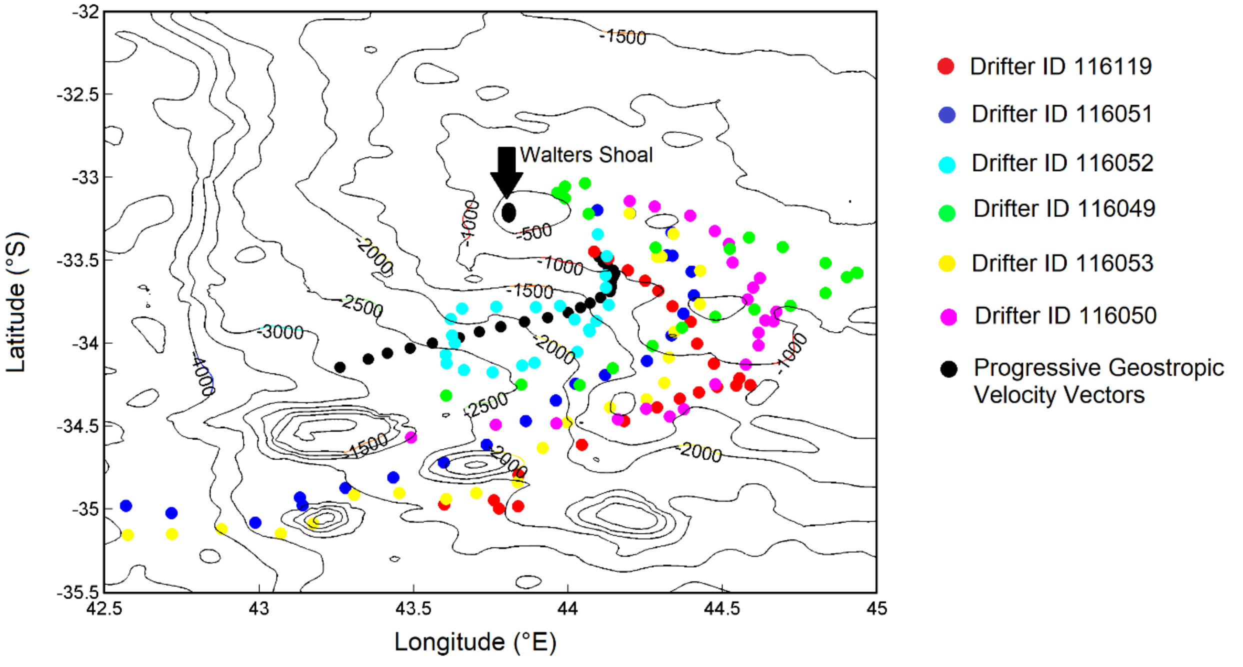

Fig. 3. Validation of satellite-derived geostrophic currents near Walters Shoal using 6 SVP drifters (coloured tracks) and a geostrophic-derived progressive vector plot (black dots). The tracks are for 24 days. The geostrophic progressive vector (virtual) trajectory follows the tracks of the actual SVP drifters very well but travels a smaller distance.

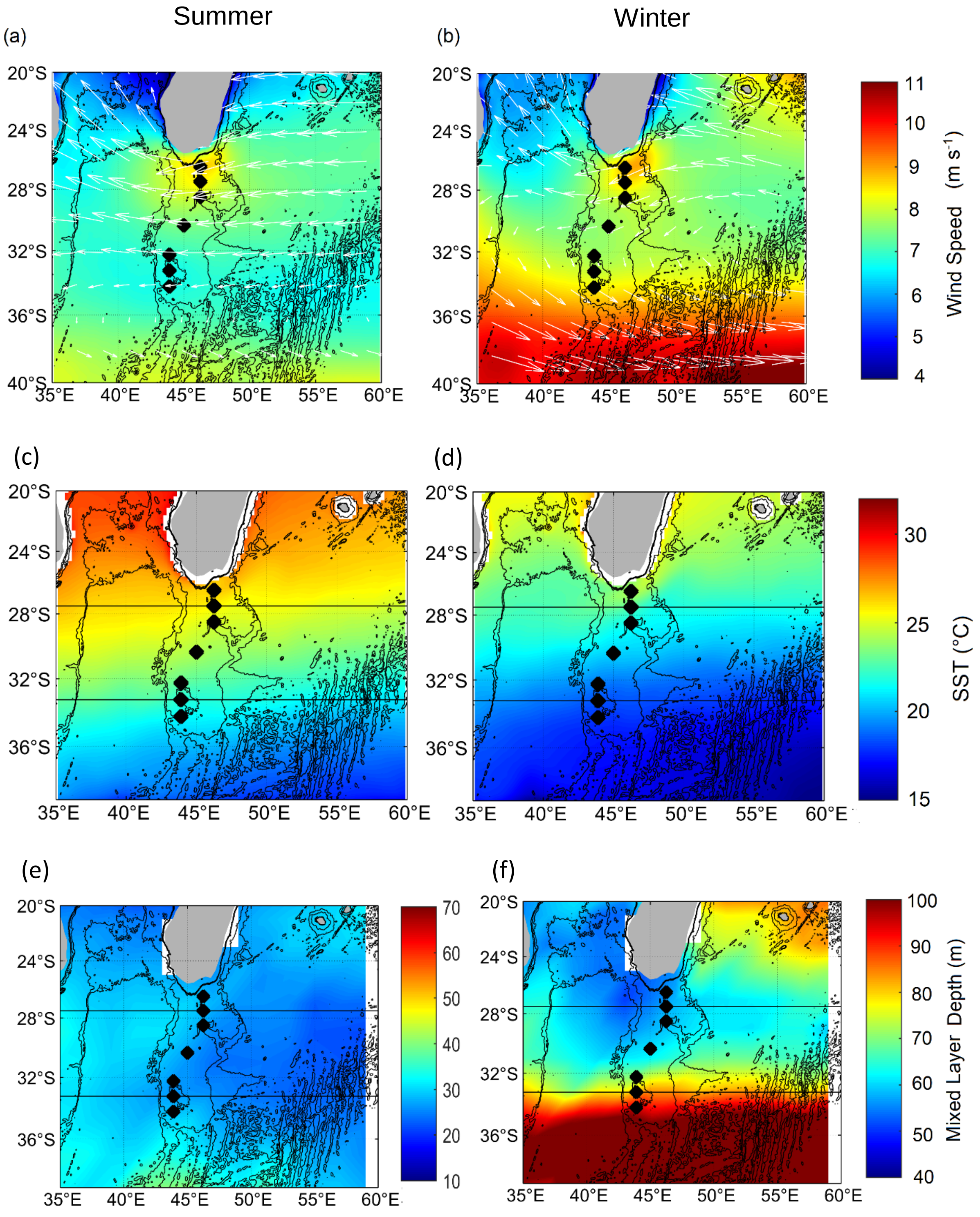

Fig. 4. Summer and winter wind field and ocean properties in the greater region of the Madagascar Ridge: (a) and (b) Surface winds, (c) and (d) SST, (e) and (f) Mixed Layer Depth, (g) and (h) Total Heat Flux, (i) and (j) EKE, (k) and (l) Chl-a. The two horizontal black lines indicate the latitudes of the MAD-Ridge pinnacle (27.5° S) and the Walters Shoal (33.25° S) whilst the black diamonds indicate the 7 virtual moorings along the Madagascar Ridge. All maps have GEBCO2014 bathymetry overlay.

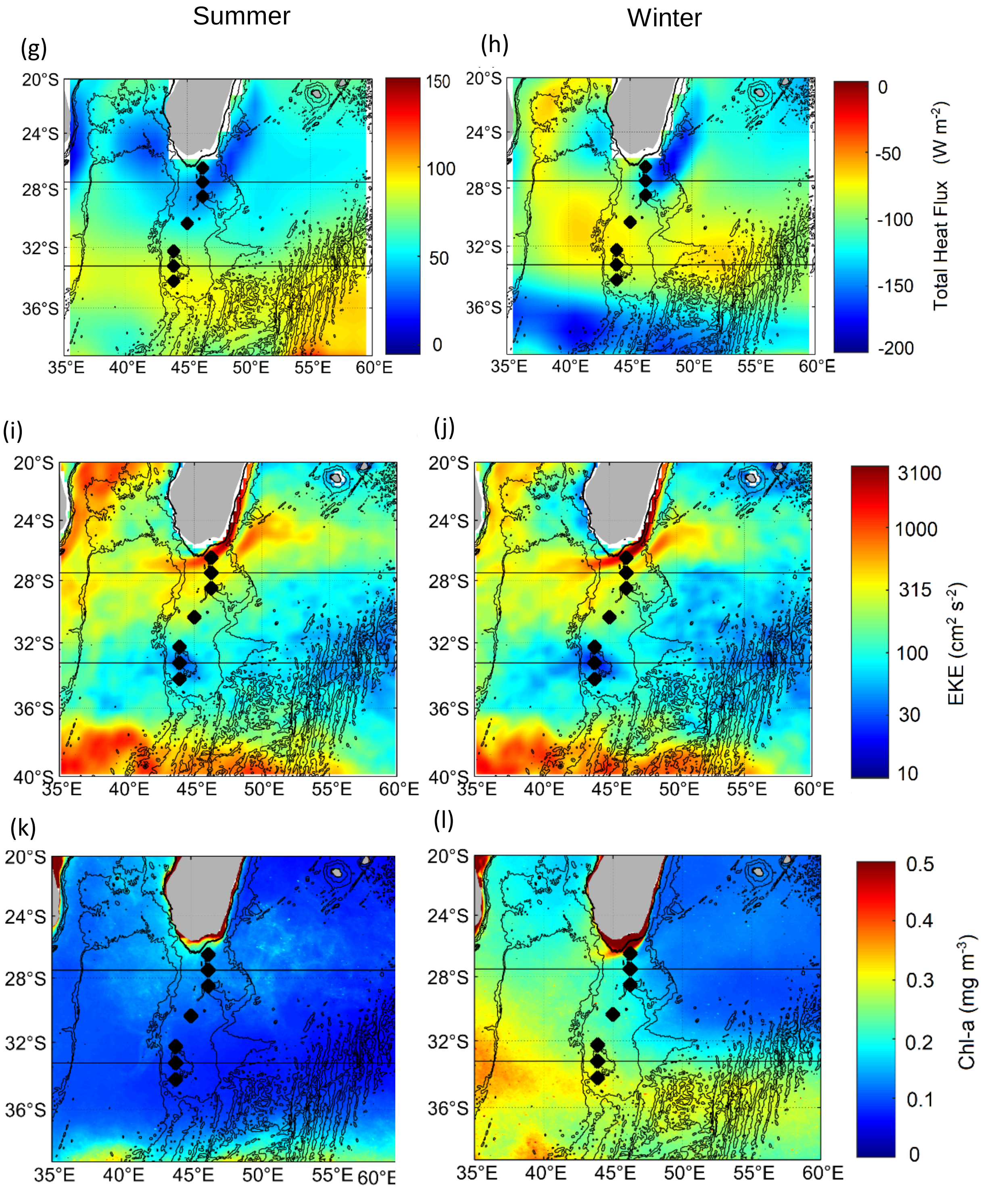

Fig. 4. (Cont.) Summer and winter wind field and ocean properties in the greater region of the Madagascar Ridge: (a) and (b) Surface winds, (c) and (d) SST, (e) and (f) Mixed Layer Depth, (g) and (h) Total Heat Flux, (i) and (j) EKE, (k) and (l) Chl-a. The two horizontal black lines indicate the latitudes of the MAD-Ridge pinnacle (27.5° S) and the Walters Shoal (33.25° S) whilst the black diamonds indicate the 7 virtual moorings along the Madagascar Ridge. All maps have GEBCO2014 bathymetry overlay.

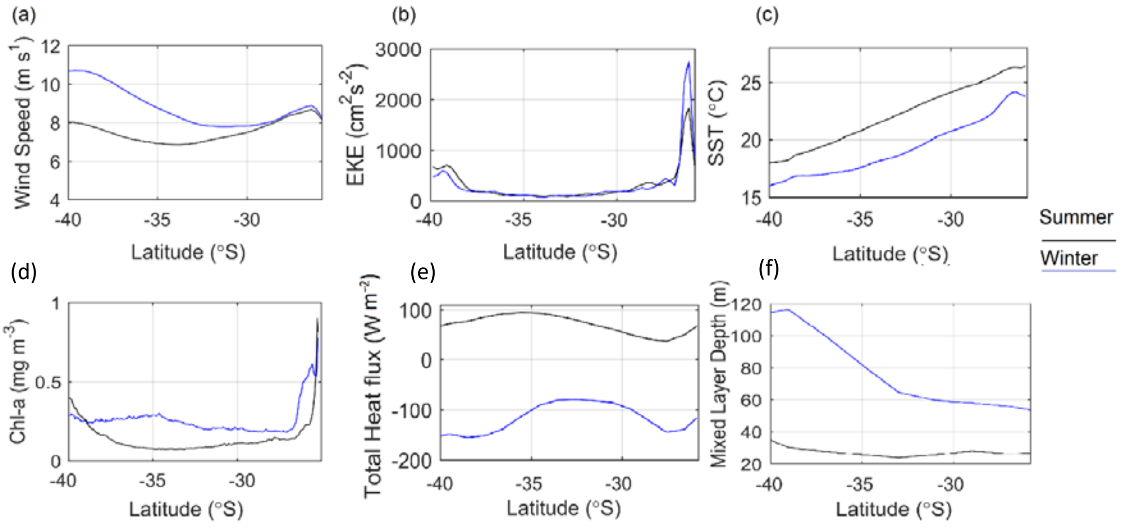

Fig. 5. Plots detailing summer (black line) and winter (blue line) gradients along the center of the Madagascar Ridge: (a) Surface winds, (b) EKE, (c) SST, (d) Chl-a, Total Heat Flux, (f) Mixed Layer Depth.

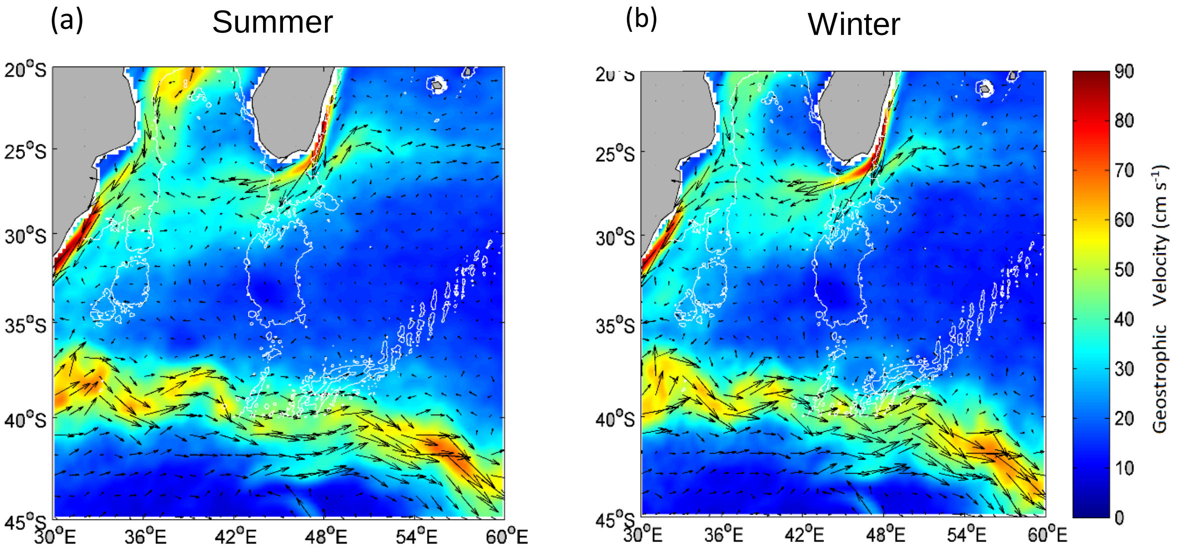

Fig. 6. Climatology of the circulation in the vicinity of the Madagascar Ridge – (a) Summer, (b) Winter. GEBCO2014 bathymetry overlay is depicted in white.

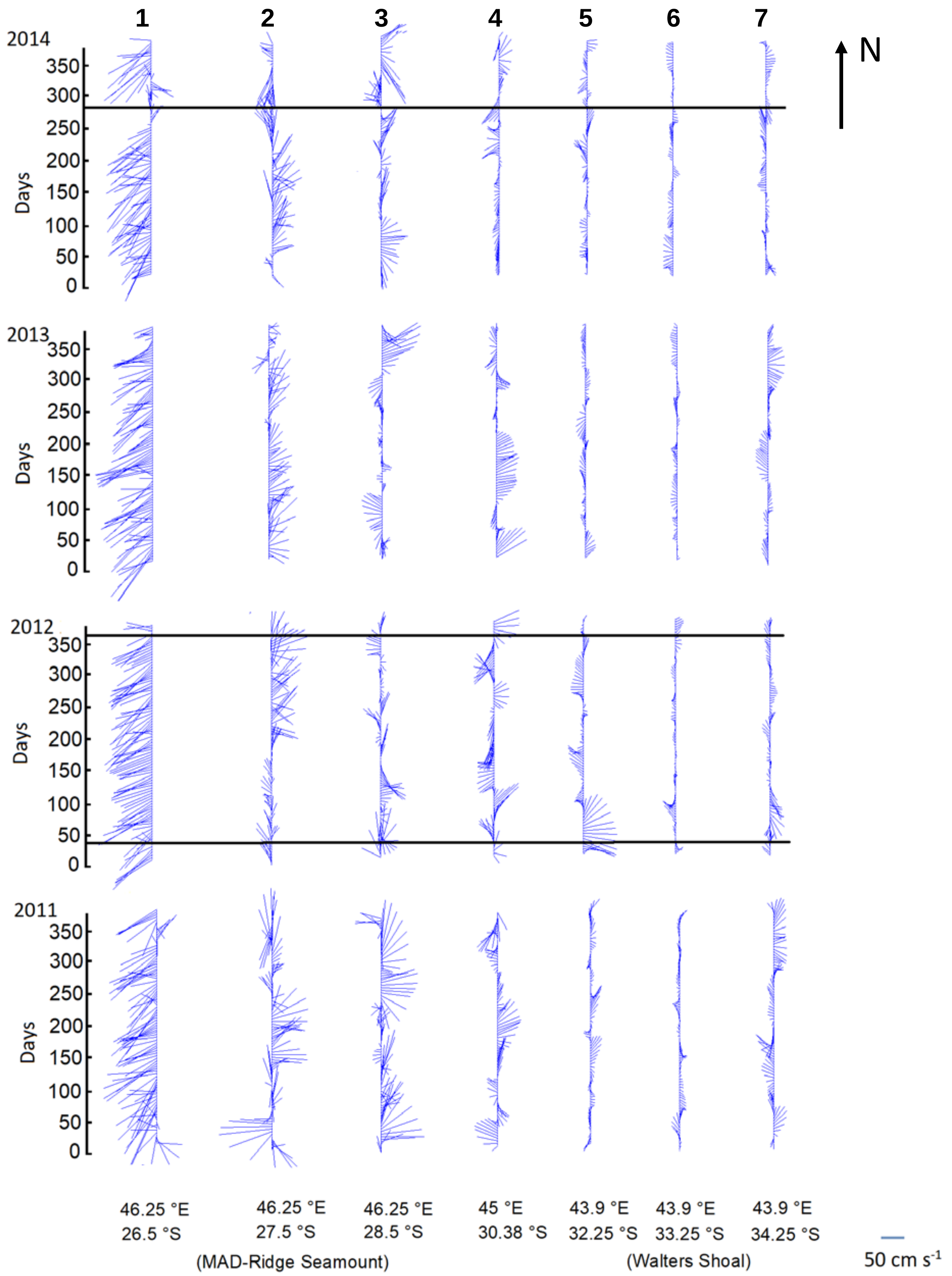

Fig. 7. Four-day time series of geostrophic currents between 2011 and 2014 for the 7 virtual mooring sites (numbered) along the Madagascar Ridge shown on Fig. 2. Black horizontal lines depict dates selected for anomalies for the specific mooring. Geostrophic velocities generally decrease from north to south with the EMC (south-westerly direction) clearly visible at virtual mooring 1.

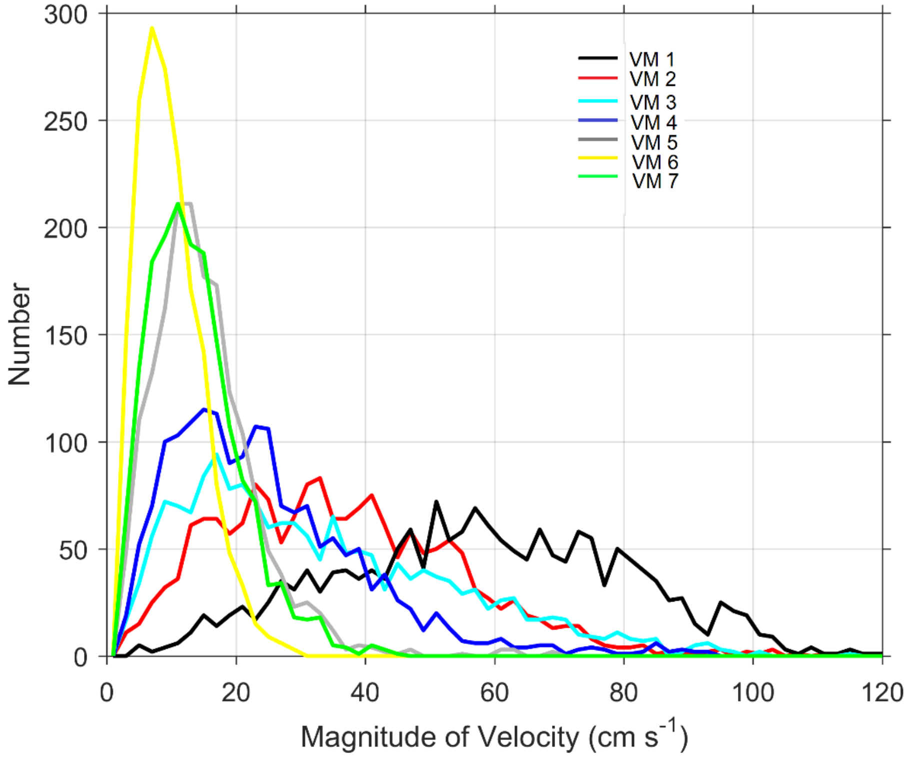

Fig. 8. Number distribution of geostrophic velocity magnitude (surface) for virtual moorings 1 - 7

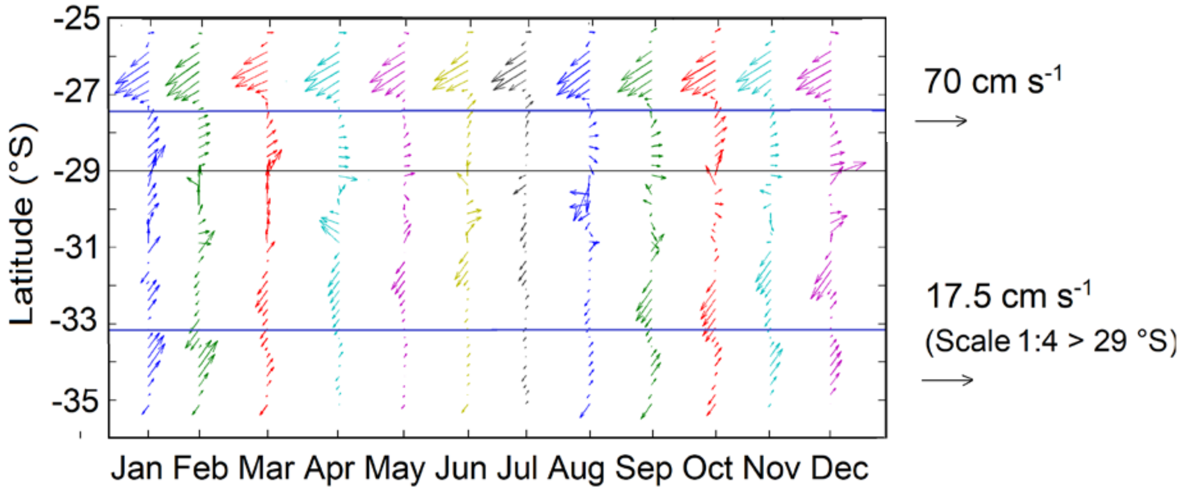

Fig. 9. Monthly mean climatology of currents across the Madagascar Ridge for the period 1993 - 2016. The two blue lines indicate the position of the MAD-Ridge pinnacle (27.5° S) and the Walters Shoal (33.25° S) whilst the black line indicates a of change of scale for current strengths indicated (right side of the diagram).

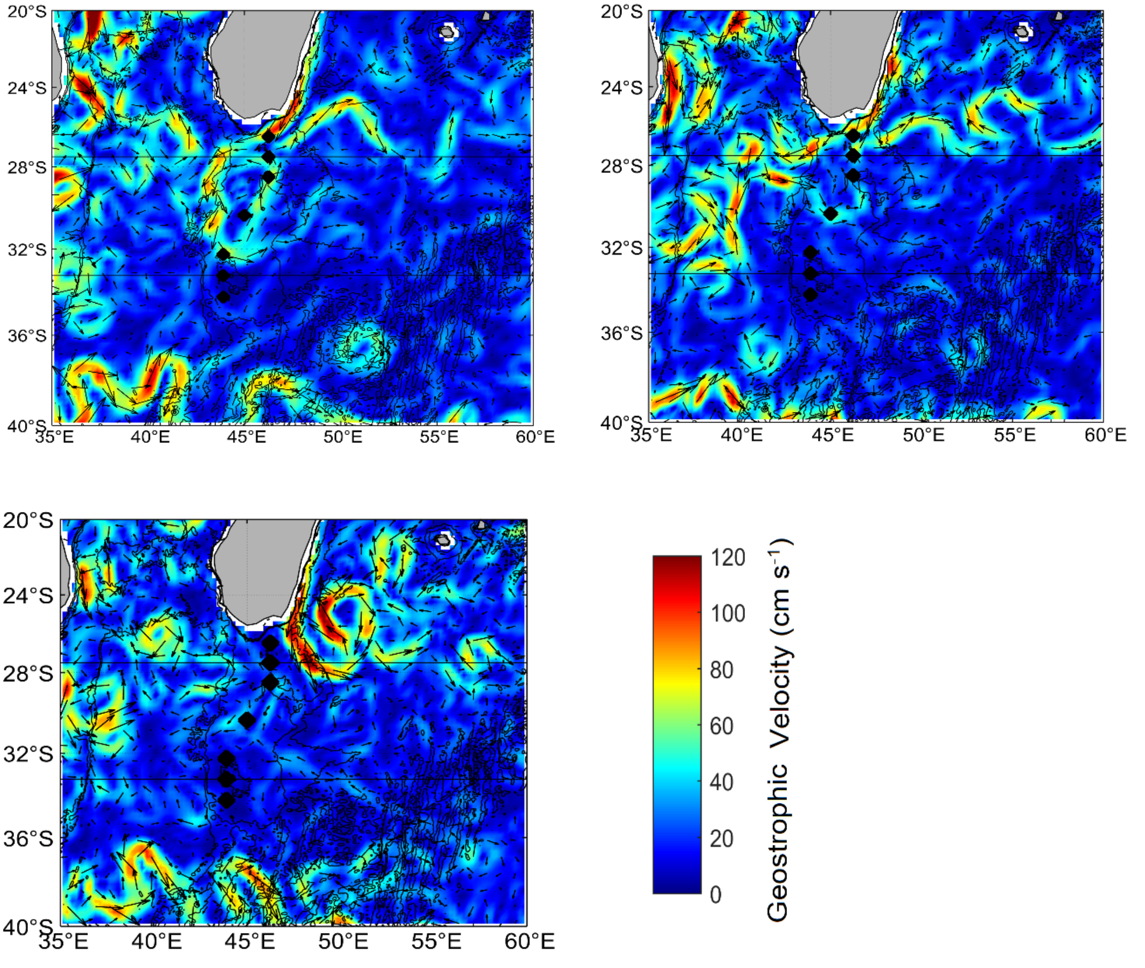

Fig. 10. Maps of horizontal geostrophic velocities highlighting anomalous events. (a) 15 January 2012, (b) 30 December 2012, (c) 27 September 2014. (a) indicates the retroflection occurring around VM 5, (b) indicates the retroflection occurring around VM 4 whilst (c) indicates an early retroflection at near the SE coast of Madagascar and VMs 1 – 3 experience lower than average geostrophic velocities. All maps have GEBCO2014 bathymetry overlay.

Author's Declaration of Interest

Regarding the submission of the research manuscript untitled:

Ocean currents and environmental gradients in the vicinity of the Madagascar Ridge in the Southwest Indian Ocean

We wish to confirm that there are no known conflicts of interest associated with this publication and there has been no significant financial support for this work that could have influenced its outcome.

We confirm that the manuscript has been read and approved by all named authors and that there are no other persons who satisfied the criteria for authorship but are not listed. We further confirm that the order of authors listed in the manuscript has been approved by all of us.

We confirm that we have given due consideration to the protection of intellectual property associated with this work and that there are no impediments to publication, including the timing of publication, with respect to intellectual property. In so doing we confirm that we have followed the regulations of our institutions concerning intellectual property.

We confirm that the work described has not been published previously, that it is not under consideration for publication elsewhere, that its publication is approved by all authors and that, if accepted, it will not be published elsewhere in the same form, in English or in any other language, including electronically without the written consent of the copyright-holder.

We further confirm that any aspect of the work covered in this manuscript that has involved experimental animals has been conducted with the ethical approval of all relevant bodies.

We understand that the Corresponding Author is the sole contact for the Editorial process (including Editorial Manager and direct communications with the office). She is responsible for communicating with the other authors about progress, submissions of revisions and final approval of proofs. We confirm that we have provided a current, correct email address which is accessible by the Corresponding Author and which has been configured to accept email from *patrick.vianello2@gmail.com*

Signed by all authors as follows:

LIST OF AUTHORS

Patrick Vianello (corresponding author)

Date 04/12/2019 Signature

Jean-François Ternon

Date 04/12/2019 Signature

Hervé Demarcq

Date 04/12/2019 Signature

Steven Herbette

Date 04/12/2019 Signature

Michael Roberts

Date 03/12/2019 Signature